Dielectric Studies of Blends of Poly(ethylene oxide) and Poly(styrene-*co*-*p*-hydroxystyrene). Semicrystalline Blends

Xing Jin, Shihai Zhang, and James Runt*

Department of Materials Science and Engineering and Materials Research Institute, The Pennsylvania State University, University Park, Pennsylvania 16802

Received February 5, 2004; Revised Manuscript Received March 31, 2004

ABSTRACT: The segmental and local dynamics of semicrystalline, melt-miscible blends of poly(ethylene oxide) [PEO] and a poly(styrene-*co*-*p*-hydroxystyrene) copolymer [SHS] were investigated using dielectric relaxation spectroscopy (DRS). A broad, yet well-defined, DRS segmental process is observed for the 5 wt % SHS blend, and it gradually shifts to higher temperature and broadens further with increasing SHS content. It can be distinguished in the 3D spectrum of the 10 wt % SHS blend, but it is only barely discernible in the spectrum of the 15 wt % SHS blend, as it is masked by large low frequency losses likely arising from electrode polarization. On the basis of current and previous findings, we propose that the observed segmental process is comprised of a slower cooperative segmental relaxation involving both components, as well as a faster process due to less associated PEO segments. Furthermore, heterogeneous spatial distribution of the SHS segments also promotes broadening of the segmental process in these blends, particularly at higher SHS contents. Hydrogen-bonded hydroxystyrene units produce a β_{S1} process, which is more cooperative than typical local relaxations, in light of its activation energy and the temperature insensitivity of its relaxation strength. All blends exhibit a high-frequency γ_b relaxation, near the γ_{PEO} and SHS β_{S2} processes of the neat components. The $f-T$ locations of the γ_b relaxation in the various blends are the same within experimental error, and they are closer to the γ_{PEO} than to SHS β_{S2} process.

Introduction

For globally miscible polymer blends with weak interactions between the component polymers and a T_g difference between the components (ΔT_g) of ≤20 K, thermorheological simplicity is expected and has been observed.[1] In addition, it has been widely recognized that the relaxation times and their temperature dependences of individual components are significantly different in many globally miscible polymer blends and disordered diblock copolymers; see, e.g., ref 2. This phenomenon is ascribed to dynamic nanoscale heterogeneities and can be detected by nuclear magnetic resonance (NMR) and dielectric and mechanical spectroscopies but not DSC due to its larger probe length scale. Nanoheterogeneities have been observed in blends with large T_g contrast, as shown in the extensive studies on blends of polyisoprene and poly(vinylethylene) (PI/PVE, $\Delta T_g \approx 60$ K)[3] and polystyrene and poly(vinyl methyl ether) (PS/PVME, $\Delta T_g \approx 130$ K).[4] These results have been explained using several models, principally concentration fluctuations,[5] chain-connectivity,[6] and intrinsic mobility differences.[7]

To elucidate the influence of strong intermolecular interactions on the cooperative segmental relaxations (CSR) in binary glass-forming mixtures, we have conducted dielectric relaxation spectroscopy (DRS) studies on a series of globally miscible polymer blends exhibiting intermolecular hydrogen bonding.[8,9] These intermolecular associations were found to suppress concentration fluctuations and couple the segmental motions of the two components. Only one CSR involving both species was observed in blends of poly(4-vinylphenol) (PVPh) with poly(ethyl methacrylate) and poly(vinyl acetate) at 10−40 wt % PVPh[9] and poly(vinyl ethyl ether) (PVEE) at 30−50 wt % PVPh.[8] This is in accord with homogeneity on a length scale of 2−3 nm, as indicated by a single composition-dependent ^{1}H $T_{1\rho}$ (proton spin−lattice relaxation time in the rotating frame) in blends where PVPh forms hydrogen bonds with the other component, such as poly(methyl acrylate)[10] and poly(ethylene oxide) (PEO).[11]

The mobility and intermolecular interactions also play an important role in determining the microstructure and crystallization behavior of semicrystalline melt-miscible blends, as demonstrated in our investigations of a series of model blends containing PEO and amorphous polymeric diluents.[12] The introduction of strong intermolecular associations between the components results in significantly reduced spherulite growth rates and facilitates diluent segregation over relatively large length scales, regardless of the diluents' mobility at the crystallization temperature. For the case of strongly interacting diluent polymers, the usual linear spherulite radius vs time ($R \propto t$) behavior slows at higher crystallization temperatures (T_c) to nonlinear growth, $R \propto t^{1/2}$. The decrease in PEO spherulite growth rates, as well as the increase in lamellar thickness, in the presence of the hydrogen-bonding miscible polymers, is mainly related to the depression of the equilibrium melting temperature of PEO in the mixtures, leading to lower degrees of supercooling. In fact, a single master curve of spherulite growth rate can be created for PEO and weakly and strongly interacting blends, by normalization via the blend T_g and degree of supercooling.

In our previous paper on amorphous blends of poly(ethylene oxide) and a 50/50 random copolymer of styrene and *p*-hydroxystyrene (SHS) with ≥60 wt % SHS,[13] despite the large T_g difference (~205 °C) between PEO and SHS, a single dominant segmental relaxation was observed for the blends, once again demonstrating

* To whom correspondence should be addressed. E-mail: runt@matse.psu.edu. Telephone: 1-814-863-2749. Fax: 1-814-865-0016.

10.1021/ma049743l CCC: $27.50
Published on Web 05/25/2004

the coupling ability of intermolecular hydrogen bonds. Blend fragility was found to increase with SHS content, reflecting the combined contribution of the components. The most interesting finding was the existence of a fast process in blends containing ≥∼80 wt % SHS. Evidence supported its assignment to a noncooperative segmental relaxation of PEO repeat units confined by the rigid SHS matrix on the nanometer length scale, having some similarities to the modified segmental dynamics of polymers in ultrathin films and polymer/layered silicate nanocomposites.[14]

In the present paper, we report on a continuation of the investigation of globally miscible PEO/SHS blends using DRS, but focusing on compositions at which a portion of the PEO has crystallized from the miscible mixture on cooling from the melt. The role of the crystalline component on modifying the relaxation behavior is highlighted.

Experimental Section

Materials. The PEO used in the present study was purchased from Polysciences. M_w and M_n are 2.2×10^5 and 5.4×10^4 g/mol, respectively, as determined from gel permeation chromatography (GPC) using dimethylformamide/0.05 M LiBr as the mobile phase. Calibration was performed using PEO standards ($M_w/M_n < 1.1$) from Polymer Standards Service USA. The SHS copolymer was obtained from Hoechst Celanese and has $M_w = 9.95 \times 10^4$ g/mol and PDI = 2.8 (polystyrene-equivalent values from GPC with THF as the mobile phase). It is composed of 50 wt % styrene and *p*-hydroxystyrene. The styrene concentration was determined by Fourier Transform Infrared (FTIR) spectroscopy, using an empirical relationship between styrene content measured from NMR and the FTIR absorbance of the 1492 and 1512 cm^{-1} bands.[15]

Blends are identified in the following text as S*w*, where *w* is the weight percentage of SHS in the blend. Solutions of the appropriate amounts of PEO and SHS in 50/50 wt % THF/$CHCl_3$ were mixed and cast onto Teflon-coated Al foil (lower SHS content) or Al foil (higher SHS content). Samples were dried at room temperature for ∼12 h to allow most solvent to evaporate, then heated in a vacuum oven with the temperature gradually increased to avoid bubble formation. After heating at a final temperature of 100 °C for 45 min, the heater was turned off and samples were maintained in a vacuum until the oven cooled to room temperature. Neat PEO powder was pressed at 100 °C for several minutes and then subjected to the same thermal history as the blends. Samples were stored in a vacuum for 1 day before the dielectric experiment.

Experimental Methods. Differential Scanning Calorimetry (DSC). All DSC measurements were performed on a TA Instruments Q-100 apparatus. The temperature and transition enthalpy were calibrated using an indium standard. Samples were heated from below 0 to 100 °C at 10 °C/min. Heats of fusion were converted to degrees of crystallinity using a perfect crystal heat of fusion for PEO of 203 J/g.[16]

Approximately 10 mg pieces were cut from DRS samples and subjected to the same thermal processing as described in the previous section, to ensure that DSC samples have the same thermal history as samples used for DRS experiments.

Fourier Transform Infrared Spectroscopy. FTIR spectra were determined using a Bio-Rad FTS-6 spectrometer with a resolution of 2 cm^{-1}. Signals of 64 scans were averaged. The 2 wt % solutions of the neat polymers and blends in 50/50 wt % THF/$CHCl_3$ were cast onto KBr windows. After most of the solvent had evaporated at room temperature, the windows were heated under vacuum at 90 °C for >12 h. FTIR samples were stored in a vacuum for 1 day after heating, before their spectra were acquired.

Dielectric Relaxation Spectroscopy. DRS spectra were collected using a Novocontrol Concept 40 broadband dielectric spectrometer. Temperature control was accomplished using a Novocontrol Quatro Cryosystem. Data were acquired in the frequency domain [0.01 Hz to 10 MHz], using 2.5, 5, or 7.5 °C increments, between −140 and +25 °C (±0.1 °C stability). The onset of PEO melting begins at temperatures above ∼25 °C, resulting in considerable spectral complexity. The minimum stabilization time at a given temperature was 1 min. Samples, having a thickness of 0.2−0.5 mm and diameter a little larger than that of the upper electrode (20 mm), were sandwiched between two plate electrodes. The sample cell was purged with N_2 during all measurements.

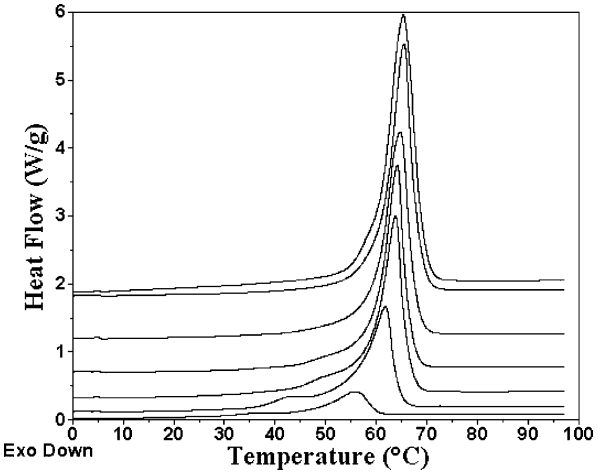

Figure 1. DSC thermograms of semicrystalline blends containing 0−40 wt % SHS. From top to bottom: PEO, S5, S10, S15, S20, S30, and S40.

Data Processing. A derivative method was used to alleviate the influence of dc loss at low frequency, especially at high temperature. Steeman and van Turnhout reported that the first derivative of frequency (f) on the dielectric constant (ϵ') provides an ohmic conduction-free dielectric loss, ϵ''_{der}:[17]

$$\epsilon_{der} = -\frac{\pi}{2}\frac{\partial \epsilon'(f)}{\partial \ln f} \tag{1}$$

A series of model calculations were conducted, and ϵ''_{der} and ϵ'' were shown to exhibit the same peak frequencies. As long as the relaxations are relatively broad (as they are in the present case), the relaxation strength of a derivative spectrum is a very good approximation to that of ϵ''.[18] The temperature location of the various relaxations (T_{max}) at individual frequencies was read from contour plots of dielectric loss (ϵ'' or ϵ''_{der}) in a 2D map of frequency vs temperature.

Results and Discussion

DSC. Figure 1 shows the DSC curves of SHS/PEO blends containing 0−40 wt % SHS, all of which exhibit PEO crystallite melting peaks but no well-defined glass transitions in the experimental temperature range. The S50 sample (not shown) did not exhibit either a melting peak or a discernible change in heat capacity associated with T_g. Overall degrees of crystallinity (X_c) and crystallinities based on the wt % of PEO in the blends are summarized in Table 1. The former decreases with increasing SHS concentration, at least partly as a result of dilution. In addition, the crystallization rate of PEO in SHS/PEO blends is slowed significantly, particularly at higher SHS contents,[12] and can also play a role in limiting crystallinity development. Crystallization was conducted on relatively slow cooling from the melt, and through 20% SHS content the PEO-based crystallinity remains high (at ∼70%, see Table 1) and remains close to that of the unblended PEO. Starting at 30 wt % SHS however, the PEO crystallinity drops rapidly to zero in the 50% SHS blend, for the crystallization conditions used here. Such behavior is commonly observed for mis-

Table 1. Degrees of Crystallinity and Fraction of PEO and SHS in the Amorphous Phase

SHS wt %	0	5	10	15	20	30	40
X_c (wt %)	79	68	63	60	56	40	11
crystallinity based on PEO fraction (%)	79	72	70	71	70	57	18
wt % of amorphous PEO	21	27	27	25	24	30	49
SHS fraction in amorphous phase (%)		16	27	37	45	50	45
estimated T_g of amorphous phase[a] (°C)	−55	−37	−22	−7	+6	+15	+6

[a] Estimated using the Fox equation[31] with PEO and SHS T_gs of −55 and +150 °C, respectively.

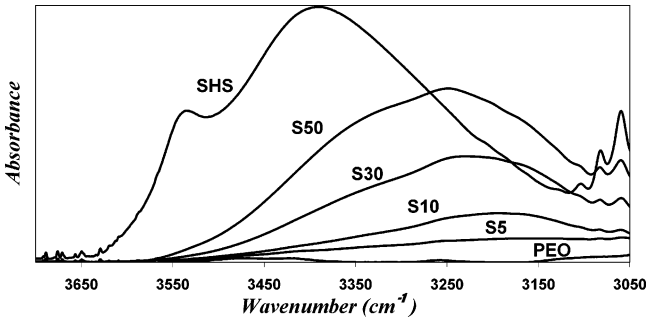

Figure 2. Room-temperature FTIR spectra of PEO and SHS blends from 3050 to 3700 cm^{-1}. Note: S50 blend is noncrystalline, but its spectrum is included here to link with the FTIR results in our previous work.[13]

cible mixtures of low T_g crystalline polymers (T_g(PEO) ∼ −55 °C) with amorphous polymer glasses.[e.g.19]

The amorphous phase composition is of course not the same as the overall blend composition due to PEO crystallinity, and the second row from bottom in Table 1 lists the SHS concentration in the amorphous phase, which increases with increasing SHS content until reaching 20% overall SHS composition and then remains approximately constant near 50% SHS until all crystallinity is lost.

FTIR. The FTIR spectra of PEO and the blends (Figure 2) are analyzed with reference to a previous FTIR investigation of PVPh/polyether blends.[20] For the S5 blend, a broad and weak absorbance appears at ∼3200 cm^{-1} and becomes more well-defined as SHS content increases to 10%. This peak is predominately associated with the SHS −OH groups *inter*molecular hydrogen bonded with PEO ether oxygen atoms. *Intra*-molecularly hydrogen-bonded SHS −OH absorb at 3390 cm^{-1}. This is in keeping with previous studies and indicates that these intermolecular hydrogen-bonded associations are stronger than SHS hydroxyl self-association.[20]

The absorbance in the −OH stretching region in Figure 2 is increasingly influenced by intramolecular hydrogen bonding with increasing SHS content, but the change in peak position is relatively small compared to that of amorphous PEO/SHS blends with SHS content >70%. (The FTIR spectra of noncrystalline PEO/SHS blends with >50 wt % SHS were described in some detail in ref 13.) Using the procedure outlined in ref 21 and the parameters displayed in Table 2 (identical to those used in ref 13), we calculate the weight fraction of SHS units in the *non-crystalline phase* that are intermolecularly hydrogen bonded with PEO, intramolecularly hydrogen bonded with other HS units, and in the unassociated state, as a function of blend composition. We assume to a first-order approximation that amorphous PEO segments are mixed more or less uniformly with the SHS. The results of these calculations are summarized in Figure 3. Note that the different hydrogen-bonding SHS fractions plotted and the composition on the *x*-axis are of that in the *non-crystalline phase*. The intramolecular hydrogen bond fraction increases regularly with SHS content, while intermolecular hydrogen bonding exhibits a maximum near ∼70% SHS. At this composition, the intermolecular hydrogen-bonded fraction begins to drop sharply and the number of free −OH begins to increase significantly. This agrees well with our previous observation that the free SHS −OH FTIR absorption emerges at ∼70% SHS.[13]

Table 2. Parameters Used to Estimate Inter- and Intramolecular Hydrogen Bond Fractions[a]

	molar vol (cm^3/mol)	solubility param $(cal/cm^{-3})^{0.5}$	structural unit mol wt (g/mol)	equilibrium const of hydrogen bond formation at 25 °C[d]		
				K_2	K_B	K_A
SHS[b]	208	10.2	240	9.4	29.8	39.3
PEO[c]	38.1	9.4	44.1			

[a] The intramolecular screening factor was set to 0.3 in all calculations. [b] For calculation of molar volume and unit molecular weight, the SHS structural unit was considered to contain one hydroxystyrene unit and the appropriate number of styrene units based on copolymer composition. The molar volume and solubility parameter of SHS were obtained using the volume average of those of polystyrene and PVPh. The PVPh data used were those in ref 32 and the PS data were calculated in the same manner as PEO (see footnote *c*). [c] The PEO molar volume and solubility parameter were calculated using a group contribution method, and the data from the Penn State Data Bank. [d] Equilibrium constants: K_2, for SHS intramolecular dimer formation; K_B, for SHS intramolecular multimer formation; K_A, for the intermolecular hydrogen bonding between PEO and SHS. Corresponding enthalpy of hydrogen bond formation: $h_2 = -5.60$, $h_B = -5.20$, and $h_A = -5.4$ kcal/mol.

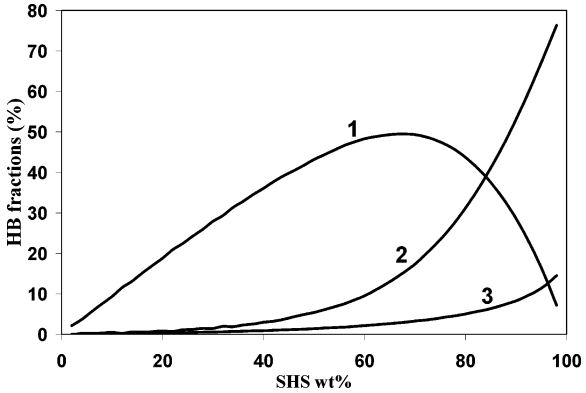

Figure 3. Calculated hydrogen-bonding (HB) fractions as a function of blend composition. Key: curve 1, fraction of SHS intermolecularly hydrogen bonded with PEO; curve 2, fraction of intramolcularly hydrogen-bonded SHS; curve 3, fraction of "free" −OH.

DRS. Component Polymers. The dielectric spectra of the amorphous SHS copolymer exhibit a segmental relaxation (α_S) and two sub-T_g transitions (β_{S1}, β_{S2}).[13] Below its melting point, PEO (Figure 4a) exhibits at least three relaxations, which are generally referred to as the α, β, and γ processes, respectively, with decreasing temperature.[22] It is important to point out that for semicrystalline PEO we refer to the segmental relax-

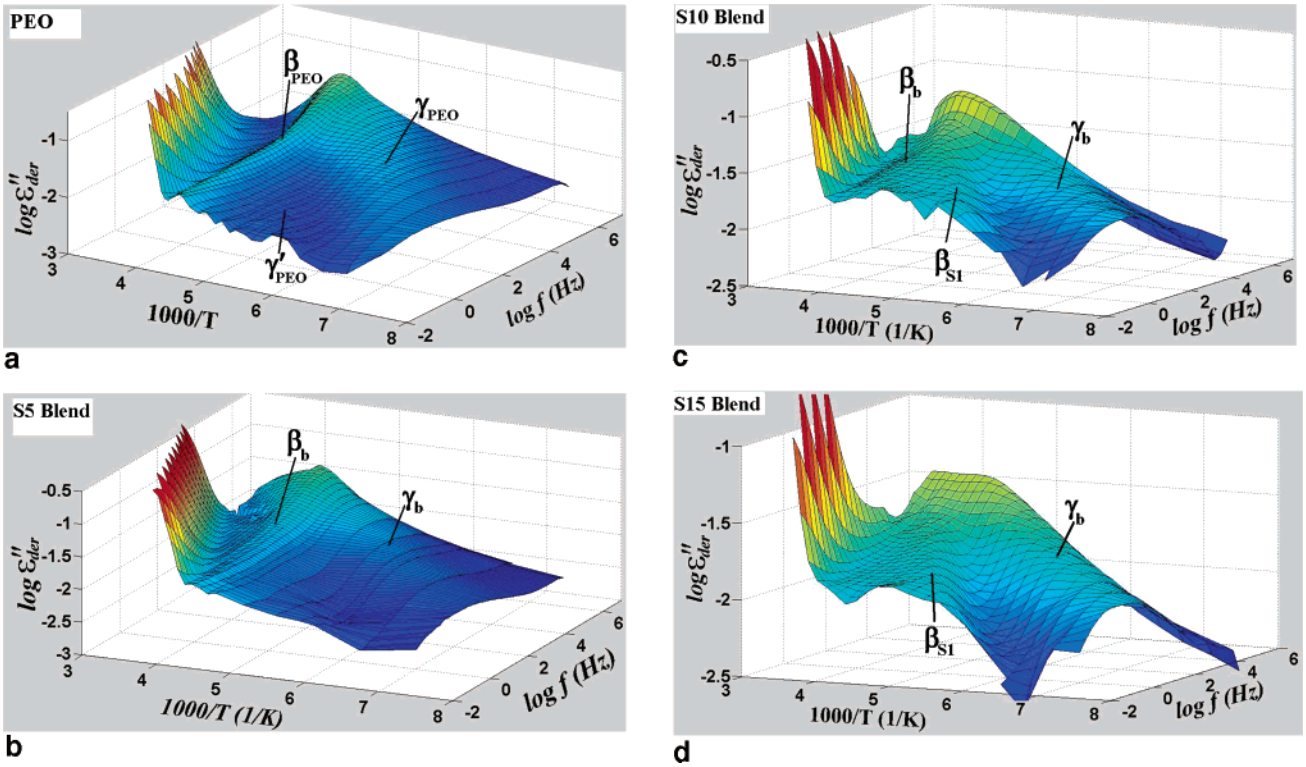

Figure 4. 3D dielectric ϵ''_{der} spectra: (a) PEO; (b) S5; (c) S10; (d) S15 blends. Data for PEO, S5 and S15 range from +25 to −140 °C, and data for S10 range from +17.5 to −140 °C.

ation as the β_{PEO} process, which originates in cooperative motions of amorphous segments. The higher temperature α_{PEO} relaxation is a process associated with the crystalline phase. The lower temperature γ_{PEO} process has been assigned to local twisting in the main chains, likely in both the noncrystalline and crystalline phases. Finally, we recently reported the observation of a relaxation between the β_{PEO} and γ_{PEO} processes, which we denoted as γ'_{PEO}.[23] The possibility of assigning the γ'_{PEO} process to Maxwell−Wagner−Sillars interfacial polarization or the presence of residual water was ruled out.[23] We suggested that this process arises from the motion of PEO segments in regions between crystalline lamellae and disordered interlamellar amorphous segments. This assignment was supported by several experimental findings: e.g., that the frequency distribution of the γ'_{PEO} relaxation becomes broader with increasing temperature and that the segmental relaxation maintains its VFT character after merging with the γ' process. The assignment also is consistent with variations in relaxation strength for samples having experienced different thermal histories. The unusual local character of the γ'_{PEO} segmental process was rationalized by analogy to the fast process or primitive segmental relaxation in nanoconfined glass-forming systems. Recently, a poly(vinyl methyl ether) (PVME) relaxation extremely analogous to the γ'_{PEO} process was observed in polystyrene (PS)/PVME blends with high PS content,[24] and confinement from the relatively rigid PS chains was proposed to have an important contribution to this relaxation.

PEO/SHS Blends. Segmental Relaxation. As seen in Figure 4b, a well-defined process (which we term β_b) occurs at relatively high temperatures and frequencies in the 3D spectrum of the S5 blend. A plot of the peak frequency vs temperature (see Figure 5, open circles at high temperature (low T^{-1})) demonstrates that the β_b process is highly temperature sensitive and displays VFT behavior. Thus, it is assigned to the segmental relaxation in the mixed amorphous phase. With the involvement of SHS segments (~16% of the amorphous phase in the S5 blend), the β_b process is naturally located at higher temperatures than the β process of neat PEO (compare data in Figure 5). The 3D DRS spectrum of the S5 blend (Figure 4b) maintains the general characteristics of that of neat PEO (Figure 4a), except that all dispersions become significantly broader. The broadening of the CSR process of the S5 blend compared to that of neat PEO is more clearly seen (qualitatively) by comparing their 2D isochronal DRS spectra in Figure 6.

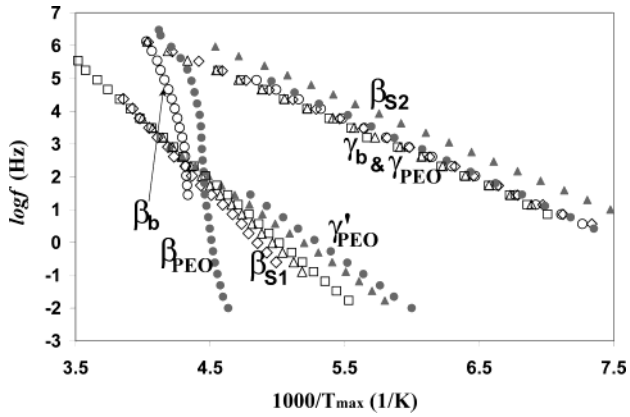

Figure 5. Arrhenius plot of the peak frequency−temperature ($f-T$) for various relaxations in semicrystalline blends, compared with those of the component polymers. Filled labels: neat components (triangle, SHS; circle, PEO). Empty labels: blends (circle, S5; diamond, S15; triangle, S30; square, S40).

Previously, despite strong intermolecular coupling, two segmental relaxations were observed for globally miscible amorphous blends of poly(vinyl ethyl ether)

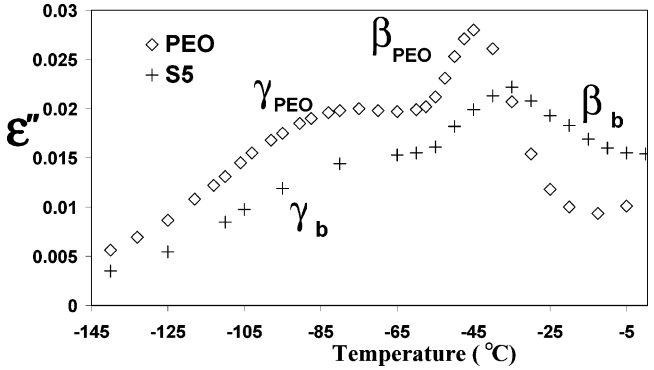

Figure 6. Isochronal DRS spectra of neat PEO and the S5 blend at 1.2×10^4 Hz.

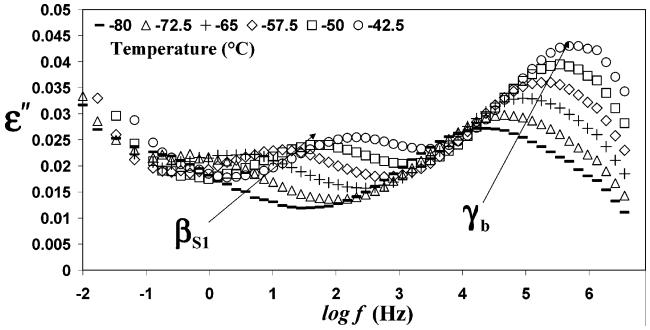

Figure 7. Low-temperature dielectric loss spectra of the S40 blend.

[PVEE] with poly(vinylphenol) (= poly(*p*-hydroxystyrene) [PVPh]) with <30 wt % PVPh, due to a simple hydrogen-bonding stoichiometric effect.[8] The slower of these two processes arises from hydrogen-bonded PVPh and PVEE segments and the faster from "free" (unassociated) PVEE segments. A similar stoichiometric effect was also observed for amorphous PVEE/SHS blends.[25] In light of the similarity between the chemical structures of PVEE and PEO, it is reasonable therefore to propose that at least part of the increased breadth of the β_b process in SHS/PEO blends at low SHS content arises from the existence two CSR processes. In addition, SHS significantly reduces the crystallization rate of PEO in the blends, permitting the diffusion of SHS molecules away from the crystal growth front, over relatively large length scales.[12] This can result in a rather heterogeneous spatial distribution of the amorphous segments (from interlamellar to interfibrillar environments) and can also contribute to broadening of the loss frequency distribution of the β_b relaxation.

The β_b process gradually shifts to higher temperatures and broadens upon increasing SHS content from 5 to 10% (Figure 4, parts b and c). On the basis of the estimated T_g of the amorphous portion of the S15 blend (see Table 1), its β_b relaxation is expected to reside in the experimental frequency−temperature ($f-T$) range (Figure 4d). However, following the behavior of the S5 and S10 blends, its β_b relaxation is expected to be quite broad and, moreover, it is dominated by large low frequency losses, which likely arise from electrode polarization. Therefore, the β_b is only just discernible in the spectrum of the S15 blend,

Finally, the γ'_{PEO} process of neat PEO (Figure 4a) essentially disappears in the DRS spectrum of the S5 blend, and this region of the spectra is progressively dominated by the local β_{S1} relaxation for blends with 10 wt % SHS and above (see below). It is conceivable that the diffuse nature of the γ'_{PEO} process after addition of only 5 wt % SHS is associated with penetration of SHS into the PEO order−disorder interphase, as predicted when strong intermolecular associations exist.[26]

***β*S1 Relaxation.** A dispersion gradually develops in the vicinity of SHS local β_{S1} relaxation and becomes well-defined at 15% SHS (Figure 4d). In light of the gradual loss of PEO-like spectral characteristics and the simultaneous development of characteristics associated with SHS, it is reasonable to conclude that this dispersion has a similar origin as that of the local β_{S1} process in neat SHS, and therefore is labeled as β_{S1} in Figure 4, parts c and d. In the $f-T^{-1}$ plot in Figure 5, only β_{S1} data for neat SHS, S15, S30, and S40 blends are presented for clarity. Although the β_b and β_{S1} processes are evident in the 3D DRS spectrum of the S10 blend (Figure 4c), it is difficult to define reliable peak $f-T$ locations, and S10 data points are therefore not provided in Figure 5.

Analogous to the findings for the secondary relaxations of poly(allyl alcohol) and some polysaccharides,[27] we proposed in an earlier paper that the SHS β_{S1} relaxation was associated with hydroxystyrene units that are hydrogen bonded: either self-associated in neat SHS or inter- and intramolecularly hydrogen bonded in associating blends.[13] As seen in Figure 5, the slope of the β_{S1} $f-T^{-1}$ data gradually decreases with increasing SHS content, i.e., the apparent activation energy (E_a) decreases. $E_a(\beta_{S1})$ decreases monotonically from ~85 to 55 kJ/mol upon increasing the SHS content from 15 to 100%. [The dielectric relaxation dynamics of amorphous SHS/PEO blends having >50 wt % SHS were reported in a previous publication.[13]] This is consistent with weaker SHS intramolecular self-associations dominant at higher SHS content, compared with stronger intermolecular hydrogen bonding between SHS and PEO which dominates at higher PEO contents. Changes in the $f-T$ locations of local processes with blend composition are not often observed, but similar findings have been reported for semicrystalline poly(vinylidene fluoride)− [PVDF] poly(methyl methacrylate) [PMMA] blends, in which the PVDF local relaxation clearly shifts with composition and the local PMMA β process also shifts, but to a lesser extent.[28]

The above values of activation energy (E_a) for the β_{S1} process (~85−55 kJ/mol) are higher than those of typical local relaxations (20−50 kJ/mol[29]) but well below the apparent E_a of typical segmental processes. The relaxation strength ($\Delta\epsilon$) of noncooperative local processes increases with increasing temperature, due to increased dipole fluctuation angle and fraction of mobile groups. This is precisely what is found for the local γ_b processes of the blends (see Figure 7). In contrast, the strength of the β_{S1} relaxation is nearly insensitive to temperature (although the apparent peak loss increases as it begins to overlap with the γ_b process at higher temperatures). Both observations indicate that the β_{S1} process is more cooperative than typical local processes. For neat SHS, due to the larger separation between the $f-T$ locations of the segmental and β_{S1} processes, the influence of the former on the low-frequency side of the latter is negligible.[13] Consequently the temperature insensitivity of the β_{S1} relaxation strength, and hence the relatively greater cooperative nature of the β_{S1} process, is more convincingly indicated in neat SHS.

γ_b Relaxation. As noted above, all blend DRS spectra exhibit a low temperature, high-frequency relaxation (γ_b, see Figure 5) near the γ_{PEO} (filled circles) and SHS β_{S2} processes (filled triangles) of the neat components. The $f-T$ locations of the γ_b process in the various crystalline and noncrystalline (the latter were studied previously[13]) PEO/SHS blends are the same within experimental error and are closer in shape and location to γ_{PEO} than to the SHS β_{S2} process.

For semicrystalline blends, the isothermal dielectric loss spectra at −125 °C were fit with a Havriliak−Negami (HN) function and a dc loss contribution:[30]

$$\epsilon(\omega) = \epsilon' - i\epsilon = \frac{\epsilon_0 - \epsilon_\infty}{(1 + (i\omega\tau)^a)^b} + \epsilon_\infty - i\left[\frac{\sigma}{\epsilon_V \omega}\right]^s \quad (2)$$

where ϵ_∞ and ϵ_0 are the limiting dielectric constants at high and low frequencies, respectively ($\epsilon_0 - \epsilon_\infty = \Delta\epsilon$, the relaxation strength); ω is the angular frequency, τ the characteristic relaxation time, σ the conductivity, and ϵ_v the vacuum permittivity, 8.85×10^{-12} F/m, and s characterizes the conduction process. The exponent s was found to be ∼0.5 in the present investigation. The exponents a and b ($0 < a, b < 1$) represent the breadth and asymmetry of the relaxation in question. Making the reasonable simplification that the γ_b process is symmetrical[29] ($b = 1$), a is found to be ∼0.31 for all blends. $\Delta\epsilon(\gamma_b)$ gradually increases with increasing SHS content (from 0.13 for PEO to 0.27 for the S40 blend), in keeping with the reduction in the overall degree of crystallinity.

Summary

Melt-miscible SHS/PEO blends containing up to 40 wt % SHS are semicrystalline under the crystallization conditions used in the present study. Through 20% SHS content, the PEO-normalized crystallinity remains close to that of neat PEO, but decreases rapidly with further increase in SHS content and reaches zero at ∼50% SHS. SHS concentration in the amorphous phase increases with increasing SHS content until the overall blend composition reaches ∼20% SHS and then remains approximately constant near ∼50% SHS until all crystallinity is lost.

The DRS cooperative segmental relaxation associated with the amorphous phase of the blends gradually shifts to higher temperatures and broadens with increasing SHS content, becoming unobservable in the spectra of semicrystalline blends with SHS concentration >15%. Its broadening is considered to arise from two factors: the presence of two segmental processes due to hydrogen-bonding stoichiometric effects and heterogeneous spatial distribution of amorphous segments.[12]

The apparent activation energy of the β_{S1} process in SHS and the blends (both crystalline and amorphous) decreases monotonically from ∼85 to 55 kJ/mol upon increasing the SHS content from 15% to 100%. This is consistent with the different strengths of the inter- and intramolecular hydrogen bonds, the fractions of which change with amorphous phase composition. The activation energy of the β_{S1} process is higher than those of typical local relaxations and its relaxation strength is almost insensitive to temperature. These observations suggest that this process has more cooperative character than typical local relaxations.

Acknowledgment. The authors would like to express their appreciation to the National Science Foundation, Polymers Program (DMR-0211056), for support of this research.

References and Notes

(1) (a) Alegria, A.; Elizetxea, C.; Cendoya, I.; Colmenero, J. *Macromolecules* **1995**, *28*, 8819. (b) Pathak, J. A.; Colby, R. H.; Kamath, S. Y.; Kumar, S. K.; Stadler, R. *Macromolecules* **1998**, *31*, 8988.

(2) (a) Quan, X.; Johnson, G. E.; Anderson, E. W.; Bates, F. S. *Macromolecules* **1989**, *22*, 2451. (b) Miller, J. B.; McGrath, K. J.; Roland, C. M.; Trask, C. A.; Garroway, A. N. *Macromolecules* **1990**, *23*, 4543. (c) Schmidt-Rohr, K.; Clauss, J.; Spiess, H. W. *Macromolecules* **1992**, *25*, 3273.

(3) (a) Arbe, A.; Alegria, A.; Colmenero, J.; Hoffmann, S.; Willner, L.; Richter, D. *Macromolecules* **1999**, *32*, 7572. (b) Hirose, Y.; Urakawa, O.; Adachi, K. *Macromolecules* **2003**, 36, 3699.

(4) (a) Pathak, J. A.; Colby, R. H.; Floudas, G.; Jérôme, R. *Macromolecules* **1999**, *32*, 2553. (b) Cendoya, I.; Alegria, A.; Colmenero, J.; Grimm, H.; Richter, D.; Frick, B. *Macromolecules* **1999**, *32*, 4065. (c) Roland, C. M.; Ngai, K. L. *Macromolecules* **1992**, *25*, 363.

(5) (a) Zetsche, A.; Fisher, E. W. *Acta Polym.* **1994**, *45*, 168. (b) Kumar, S. K.; Colby, R. H.; Anastasiadis, S. H.; Fytas, G. *J. Chem. Phys.* **1996**, *105*, 3777. (c) Roland, C. M.; Ngai, K. L. *Macromolecules* **1991**, *24*, 2261.

(6) Lodge, T. P.; McLeish, T. C. B. *Macromolecules* **2000**, *33*, 5278.

(7) Chung, G. C.; Kornfield, J. A.; Smith, S. D. *Macromolecules* **1994**, *27*, 964.

(8) Zhang, S. H.; Painter, P. C.; Runt, J. *Macromolecules* **2002**, *35*, 9403.

(9) (a) Zhang, S. H.; Jin, X.; Painter, P. C.; Runt, J. *Macromolecules* **2002**, *35*, 3636. (b) Zhang, S.; Painter, P. C.; Runt, J. *Macromolecules* **2002**, *35*, 8478.

(10) Zhang, X.; Takegoshi, K.; Hikichi, K. *Macromolecules* **1991**, *24*, 5756.

(11) Zhang, X.; Takegoshi, K.; Hikichi, K. *Macromolecules* **1992**, *25*, 2336.

(12) (a) Talibuddin, S.; Wu, L.; Runt, J.; Lin, J. S. *Macromolecules* **1996**, *29*, 7527. (b) Talibuddin, S.; Runt, J.; Liu, L.-Z.; Chu, B. *Macromolecules* **1998**, *31*, 1627. (c) Wu, L.; Lisowski, M.; Talibuddin, S.; Runt, J. *Macromolecules* **1999**, *32*, 1576. (d) Lisowski, M. S.; Liu, Q.; Cho, J.; Runt, J.; Yeh, F.; Hsiao, B. S. *Macromolecules* **2000**, *33*, 4842.

(13) Jin, X.; Zhang, S. H.; Runt, J. *Macromolecules* **2003**, 8033.

(14) (a) Anastasiadis, S. H.; Karatasos, K.; Vlachos, G.; Manias, E.; Giannelis, E. P. *Phys. Rev. Lett.* **2000**, *84*, 915. (b) Ngai, K. L. *Philos. Mag.* **2002**, *82*, 291.

(15) Xu, Y. Ph.D. Dissertation, The Pennsylvania State University, 1991.

(16) Wunderlich, B. *Macromolecular Physics*; Academic Press: New York, 1980; Vol. 3.

(17) Steeman, P. A. M.; van Turnhout, J. *Macromolecules* **1994**, *27*, 5421.

(18) Wübbenhorst, M.; van Turnhout, J. *J. Non-Cryst. Solids* **2002**, *305*, 40.

(19) Runt, J.; Rim, P. B. *Macromolecules* **1982**, *15*, 1018.

(20) Moskala, E. J.; Varnell, D. F.; Coleman, M. M. *Polymer* **1985**, *26*, 228.

(21) Coleman, M. M.; Graf, J. F.; Painter, P. C. *Specific Interactions and the Miscibility of Polymer Blends*; Technomic Publishing: Lancaster, PA, 1991.

(22) McCrum, N. G.; Read, B. E.; Williams, G. *Anelastic and Dielectric Effects in Polymer Solids*; Dover Publications Inc.: New York, 1967; p 540.

(23) Jin, X.; Zhang, S. H.; Runt, J. *Polymer* **2002**, *43*, 6247.

(24) Lorthioir, C.; Alegria, A.; Colmenero, J. *Eur. Phys. J. E* **2003**, *12*, 127.

(25) Zhang, S. H.; Jin, X.; Painter, P. C.; Runt, J. *Macromolecules* **2003**, *36*, 5710.

(26) Kumar, S. K.; Yoon, D. Y. *Macromolecules* **1991**, *24*, 5414.

(27) (a) de la Rosa, A.; Heux, L.; Cavaillé, J. Y. *Polymer* **2001**, *42*, 5371. (b) de la Rosa, A.; Heux, L.; Cavaillé, J. Y.; Mazeau, K. *Polymer* **2001**, *42*, 5665.

(28) Sy, J. W.; Mijovic, J. *Macromolecules* **2000**, *33*, 933.
(29) Schönhals, A. In *Dielectric Spectroscopy of Polymer Materials: Fundamentals and Applications*;Runt, J. P., Fitzgerald, J. J., Eds.; American Chemical Society: Washington, DC, 1997; p 107.
(30) Havriliak, S., Jr.; Havriliak, S. J. *Dielectric and Mechanical Relaxation in Materials: Analysis, Interpretation, and Application to Polymers*; Hanser Publishers: Cincinnati, OH, 1997.
(31) Fox, T. G. *Bull. Am. Phys. Soc.* **1956**, ser.2, 1, 123.
(32) Serman, C. J.; Xu, Y.; Painter, P. C.; Coleman, M. M. *Polymer* **1991**, *32*, 516.

MA049743L